6-1-2012

Sensitive Fluorescence Detection using a Camera from the Gaming Industry

Brian L. Van Hoozen Jr.
Lawrence University, blv23@cornell.edu

Sensitive Fluorescence Detection using a Camera from the Gaming Industry

Brian Van Hoozen, Jr.

Table of Contents

	Pages
Preface	3-4
I. The Role of Imaging in Fighting Cancer	5-8
II. How Video Game Technology can Help Fight Cancer	8-11
III. Theory	12-17
IV. Calibration	17-21
V. Fluorescence Imaging	22-26
VI. Conclusion	26-27
Acknowledgments	27
References	28-29
Appendix	30-31

Preface

This paper highlights the symbiotic relationship between industry and basic research. Often basic research results in discoveries that allow for the innovation of new technology by industry. In turn this new technology, provided by industry, produces new or more economically accessible instruments for conducting basic research. One recent technological example of this phenomenon is the Blu-ray disk player. Its advantage over conventional DVDs stems from using 405 nm blue lasers as opposed to 650 nm red lasers which are used in DVD players. This shorter wavelength light allows more data to be encoded onto a disk and hence better picture quality. Prior to this particular application of the blue laser, very few blue lasers existed and the few that did were expensive, difficult to acquire and cumbersome to work with. Blu-ray disk players allowed an economical means for industry to develop and optimize the production of blue lasers. Now blue lasers are mass produced so cheaply they can be incorporated into consumer electronics. Consequently, basic research that requires a blue laser can be done much more easily and cheaply than before the invention of the Blu-ray disk player.

This paper explores how another type of recently developed technology could catalyse basic research and how this basic research could provide proof of principle for a serendipitous technological application. This type of technology is known as time-of-flight imaging technology. It was originally developed for motion sensitive video gaming applications. However, the basic research I did on this camera explores how this technology could be applied to fluorescence imaging, a flourishing topic in modern scientific research. [1-4] A specific application I have explored for this technology is the imaging of fluorescently labelled tumors, a

new technique for identifying tumors in surgery. Because this technology was originally developed for the video game market, it can be produced relatively cheaply allowing for the possibility of producing less expensive medical imaging devices and consequently lower health care costs when these instruments are used. Hence, like the Blu-ray disk player, this technology shows the potential to stimulate basic research by providing a means for fluorescence imaging. This basic research can explore another application of this technology which could provide industry with a proof of principle for building new medical imaging devices. This paper explores the feasibility of this technological metamorphosis.

I. The Role of Imaging in Fighting Cancer

Along with radiation treatments and chemotherapy, the surgical removal of tumors remains one of the primary techniques physicians use to treat cancer. Often one or more of these techniques are combined to treat an individual patient[5]. Since an individual cancer cell can grow into an arbitrarily large tumour, often surgery is used to remove all of the tumors that can be found, and then chemotherapy is used to treat the few small tumors that remain[6]. Chemotherapy however, is notoriously difficult on the patient. Since chemotherapy uses drugs that disrupt rapid cell division, rapidly dividing cancer cells are killed, but so are other cells that rapidly divide under normal circumstances such as those found in hair follicles, bone marrow and the digestive tract. The death of these cells results in numerous adverse side effects for the patient such as suppression of the immune system, lowering of blood platelet count, and hair loss.[7] Studies have shown that chemotherapy is more successful and of shorter duration when preceded by a surgery that removed a larger amount of the total cancerous tissue in the body. This results in an overall better prognosis for the patient[8.] Therefore, removing as much cancerous tissue as possible is of the utmost importance for ensuring that cancer patients receive the most successful and least problematic treatment.

Identifying cancerous tissue is often non-trivial. The degree of difficulty varies with the type of cancer. Ovarian cancer is one of the most notoriously difficult. Due to the degree of difficulty, much research has been conducted in recent years investigating a technique in which the tumors are labeled with fluorescent dye so they can be identified much more easily. Recently, this technique has been applied in a handful of ovarian cancer surgeries[6]. These

fluorescent dyes are injected into the patient two hours prior to surgery and utilize a folate receptor to concentrate in the cancerous tissue. Because the fluorescence pathways of these dyes are in the visible spectrum, the tumors light up when exposed to a diffused visible light laser beam during surgery[6]. Prior to the invention of this technique, the smallest tumors that could be readily detected by eye were 3 mm in diameter; however, with this technique, physicians are able to identify tumors as small as 100 microns across.[8]

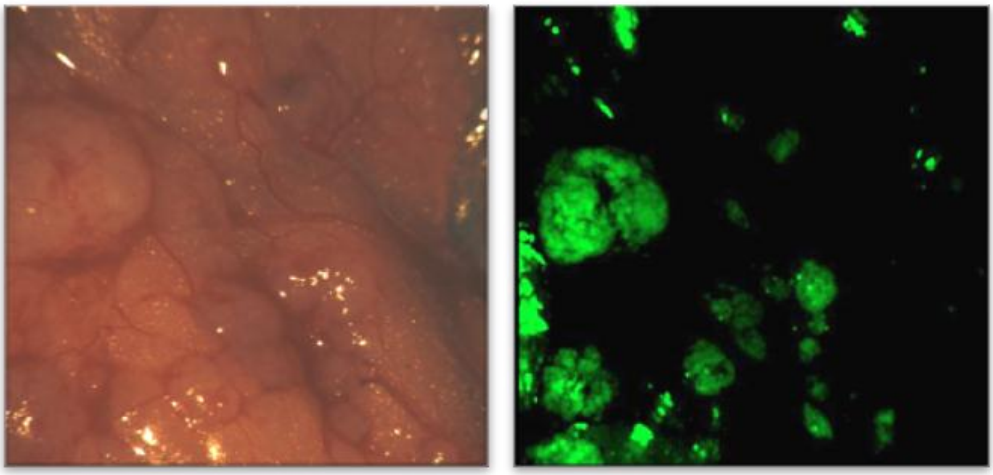

Figure 1: Both of these images are from an ovarian cancer surgery. The image on the left is the surgeon's current unassisted view of the tissue. In this image picking out the tumors is rather difficult. The image on the right is the fluorescence image of the same tissue. In this image not only are the large tumors much easier to distinguish from the rest of the tissue, but a number of smaller tumors can now be found that would otherwise have been undetectable. This figure is adapted from reference 6.

One of the difficulties surgeons still face in the operating room (even with the introduction of this technique) is that only tumors at or near the surface of the tissue can be

imaged. Visible light does not penetrate far into the tissue. Some tumors have unusual branches and twists that run deep into the tissue. To find these hidden tumors, one needs a detection technique that can penetrate further into the bulk of the tissue. This allows a surgeon to identify a tumor that is deeply imbedded into the tissue and to cut through tissue to remove it. This desire for imaging beyond the surface motivated the search for an infrared fluorescent dye[9] that could replace the previously used visible light fluorescent dye because infrared light is capable of penetrating further into the tissue than visible light. Although we cannot see infrared light, the type of infrared light emitted by this dye (750-900 nm) can easily be imaged with cameras that use standard silicon based detector chips. On the surface using light that the human eye cannot see may seem to be a setback; however, endoscopic surgeries (which require a camera anyway) [*] are becoming more prevalent in managing ovarian cancer[10]. This is because endoscopic surgeries are minimally invasive and consequently result in a shorter and less painful recovery for the patient[11]. By using endoscopic cameras to capture the infrared fluorescent signal, the deep-tissue tumors can be visualized.

The subject of this paper is the technology a potential endoscopic camera could use to detect the infrared fluorescence signal of the smallest tumors possible considering the constraints of a camera that is used in an endoscope. One can list a number of different properties that would be ideal for a fluorescence endoscopic camera. Some of the principle ones include: being able to see the fluorescence image and the conventional white light image at the same time so the surgeon does not lose any information but gains the information from

[*] Endoscopic surgery is performed using a flexible tube that is inserted into a cavity or a small incision as oppose to conventional "open surgery" where the incision has to be large enough for the physician to view the area of the operation. Some endoscopes use fiber optics to lead the signal to a camera outside of the endoscope.

the infrared fluorescence signal, being small enough in size so that it could fit in an endoscope, and being able to successfully image a fluorescence signal.

The strength of a fluorescence signal (i.e. the fluorescence signal to noise ratio) is determined by a number of different parameters. For one, the amount of fluorescent dye present in the tissue will determine the strength of the signal. However due to the toxicity of the dyes being used, the amount of dye that can be safely injected into the patient is limited. Another way to increase the fluorescence signal to noise ratio is to increase the amount of light used to excite fluorescence. However, exposing the internal organs to high optical power both is technologically more difficult (in such a small space) and is potentially harmful to the organs. A third way to increase the fluorescence signal to noise ratio is to increase the sensitivity of the camera used. This paper addresses the possibility of a new technology originally developed for video gaming applications that would have a surprising level of sensitivity for this endoscopic application.

II. How Video Game Technology can Help Fight Cancer

Over the past few decades the video game industry has grown substantially with revenues exceeding 74 billion dollars in 2011[12]. As the industry has grown, so has the economic incentive to develop new technologies for gaming. One of the most recent innovations in this industry is the ability of the gaming console to detect the three dimensional motion of the human body and use this information as an input for the game. This allows for a number of

appealing gaming applications. For example, this technology allows sports to be played using the actual physical activity necessary for playing the real sport as opposed to merely hitting an arbitrary series of buttons on a control. Consequently, a multitude of different motion sensitive technologies have been developed with this application in mind. One of these technologies is known as time-of-flight imaging technology [13]. Although this technology to date has not been incorporated into any mainstream video gaming system, due to the way this technology works, a possible serendipitous application of this motion sensitive gaming technology could be endoscopic fluorescence imaging.

Time-of-flight imaging technology works by measuring the phase shift between emitted and detected infrared light at a high modulation frequency. These cameras have built-in LEDs (light emitting diodes) that emit light modulated at 20 MHz (see figure 2). This light then reflects off objects in front of the camera and is detected by the camera. The camera uses a combination of an infrared bandpass optical filter and a four bin lock-in detection scheme for each of the 40k pixels to ensure that it is able to pick out what part of the total signal it receives is modulated at 20 MHz and in the infrared. The phase shift between the emitted and detected signals is then used (in conjunction with the speed of light) to calculate the distance at which the reflection occurred for all 40k pixels resulting in a distance image (see figure 3).

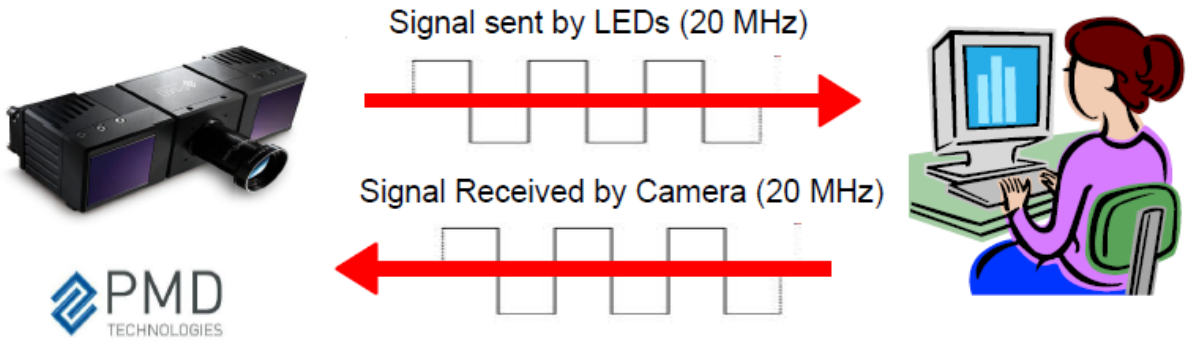

Figure 2: Time-of-Flight Camera Distance Measurement Scheme

Figure 3: Time-of-Flight Images: On the left is a distance image. Here a color scale is used to display distances with close objects labeled in red and distant objects labeled in blue. On the right is an image which displays the intensity of the infrared light reflected back to the camera. This is similar but not identical to a conventional black and white image. This figure is adapted from Reference 14.

In order to configure this camera to acquire fluorescence images (as is needed for the proposed endoscopic application), a number of modifications need to be made to the camera

(see figure 4). The electric signal originally sent to the built-in LEDs needs to be sent to a different LED of the proper power and fluorescence excitation wavelength light. A short pass filter needs to be placed in front of this LED to ensure that no photons emitted by the LED could be mistaken for fluorescence. The camera also needs the infrared band-pass filter removed and a long-pass filter placed in front of it to ensure that the camera only sees the fluorescence signal. This new configuration (see figure 4) will allow for the fluorescence signal to be detected and the non-fluorescent background to be largely suppressed. The advantage of this camera for fluorescence imaging is that the high modulation and detection frequency allows for all lower frequency noise, normally present in a fluorescence image, to be eliminated from the image. By pushing the desired signal to such a high frequency and consequently low noise regime the sensitivity of this camera to the fluorescence signal is increased substantially. As we shall see in the next chapter, not only does noise exist below the MHz regime, but in many circumstances is actually much more common at lower (<10 kHz) frequencies.

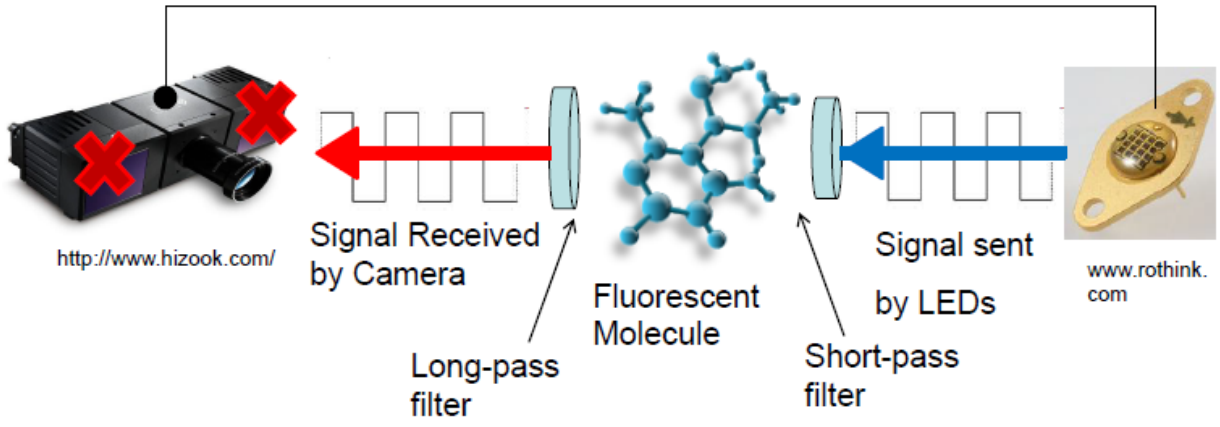

Figure 4: Fluorescence Imaging Scheme

III. Theory

A common problem with fluorescence imaging is achieving a good signal to noise ratio. Because only a small number of the excitation photons stimulate fluorescence and fluorescent photons are emitted in all directions, the optical power of the fluorescence signal can easily be three or four orders of magnitude smaller than the excitation signal. Thus being able to distinguish fluorescent photons from other (and often much brighter) sources of light is of the utmost importance for acquiring a good fluorescence image.

One way to distinguish the fluorescence signal from other sources of light is to modulate the fluorescence signal at one frequency and detect only the signal that occurs at this frequency. This is known as lock-in detection. As one might hypothesize, the amount of noise that can be eliminated with this technique is dependent on the frequency of modulation. The less common the noise is at the frequency of modulation, the better the signal to noise ratio.

Noise in an image can arise from a variety of different sources including fluorescent lights, fans, electrical interference, mechanical and acoustic vibrations and thermally generated electrons in the detector. Other than thermally generated electrons in the detector, all of these sources should have a 1/f dependence.[15] Thus the Fourier transform of the noise signal should show a 1/f dependence on the frequency until frequency independent shot noise dominates the signal (which arises from the thermally generated electrons in the detector. This is illustrated in Figure 5 which shows how even daylight contains this 1/f dependence.

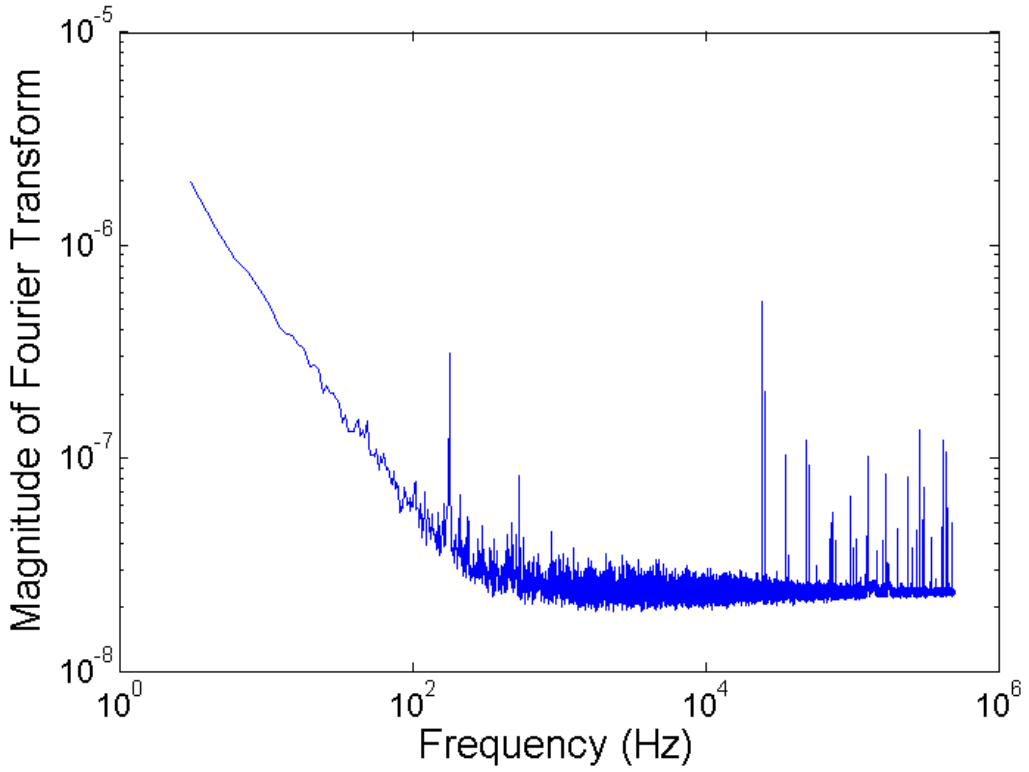

Figure 5: Fourier Transform of Daylight: On the left side of the graph, the 1/f characteristic of noise can be identified by the line of slope -1 whereas on the right side of the graph the level of noise is frequency independent which implies it is shot noise from the detector.

As shown in figure 5, noise becomes less common at higher frequencies until the shot noise limit is achieved. Thus the ability of time of flight cameras to modulate and detect light in the MHz regime offers the potential to substantially reduce the noise in a fluorescence signal by placing the signal in a regime where only shot noise is present. Although the technique of modulating fluorescence signals is not new[16], the ability of these cameras to detect at such high frequencies for 40k pixels is unprecedented.

In order to detect a signal only occurring at a specific frequency, time-of-flight cameras utilize a four bin lock-in detection scheme in which each bin collects for one fourth of the modulation period (for example 250 ns for a 1 MHz modulation). The signal is integrated for many modulation periods; however, each bin receives only a specific fourth of the modulation period as can be seen in figure 6.

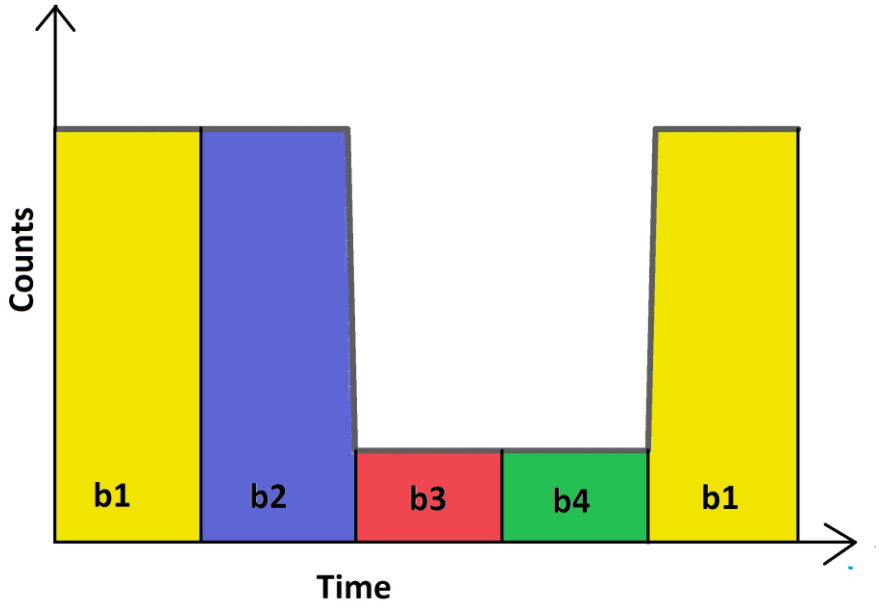

Figure 6: Four Bin Lock-in Detection Scheme: Each of the four bins collects light for one fourth of the modulation period over many periods of the modulation.

From the amount of counts collected in each bin, the signal occurring at the modulation frequency can be calculated using the equation

$$A = \frac{\sqrt{(b_2 - b_4)^2 + (b_1 - b_3)^2}}{4}$$

From the above equation, one can see that the differences between the bins 180 degrees out of phase are used as a measure of signal at the modulation frequency. To see how this subtraction technique is able to limit the noise that the camera is exposed to, we start with an equation for N modulation periods[†] in which the second half of the period τ is subtracted from the first which yields the expression

$$I_{noise} = \int_{-\infty}^{\infty} \left[\sum_{j=-\frac{N}{2}}^{\frac{N}{2}} \left[\int_{j\tau}^{\left(j+\frac{1}{2}\right)\tau} N(\omega) e^{i\omega t} dt - \int_{\left(j+\frac{1}{2}\right)\tau}^{(j+1)\tau} N(\omega) e^{i\omega t} dt \right] \right] d\omega$$

Here we assume the Fourier transform of noise N(ω) is an arbitrary function of ω which is motivated by figure 5. This equation can be reduced to

$$I_{noise} = \int_{-\infty}^{\infty} \left[\frac{4N(\omega)}{i\omega} e^{\frac{i\omega\tau}{2}} \sin^2\left(\frac{\omega\tau}{4}\right) \frac{\sin\left(\frac{N\omega\tau}{2}\right)}{\sin\left(\frac{\omega\tau}{2}\right)} \right] d\omega$$

Although, it may appear rather convoluted at first, in the high N limit the last factor in the integrand approaches the Dirac delta function in shape with the spike occurring at the modulation frequency (as can be seen in figure 7). This is multiplied by the noise Fourier transform (which is displayed in figure 5 for daylight) function meaning that only noise near the modulation frequency will be acquired and how close to the modulation frequency is necessary is determined by the number of modulation periods being integrated. For the full derivation of this equation, please see the appendix.

[†] It should be noted that this derivation assumes a two bin lock-in detection scheme (not the four bin scheme actually used by time-of-flight cameras and described in Figure 6. The derivation for four bins would just contain extra terms that would needlessly complicate the derivation without providing any additional insight as to how lock-in detection is able to suppress noise.

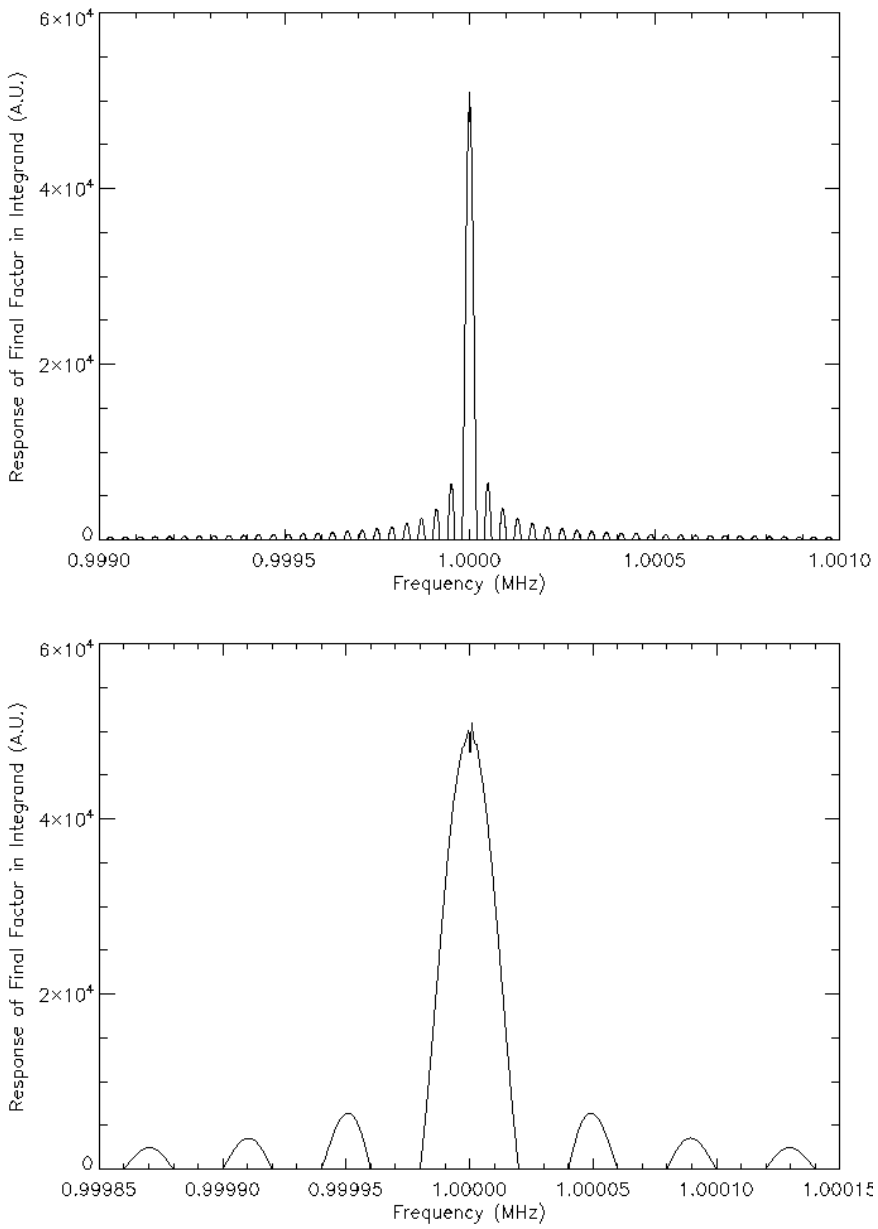

Figure 7: Graphs of the last term of the integrand: Both graphs use a modulation period of 1 μs and an integration time of 50 ms (N=50,000). The top graph is the response of this term within 1 kHz of the modulation frequency. This graph shows how the response approaches zeros as the frequency deviates from the modulation frequency. The bottom graph is a plot of the function within 150 Hz of the modulation frequency. This graph

demonstrates how the width of the largest peak is the inverse of the integration time (20 Hz in this case).

In summary, this equation demonstrates that only a small quantity of noise in the vicinity of the modulation frequency will be acquired when this modulation technique is applied. Due to the modulation frequency being so high, much more common lower frequency noise (demonstrated in figure 5) can be eliminated from the signal. In the next chapter, this theoretical hypothesis will be tested by analyzing how this technique impacts the amount of noise in the signal.

IV. The Calibration

Two different experiments were conducted. In both experiments the time-of-flight camera tested was a PMD[vision]® CamCube 3.0. This chapter discusses the calibration of this camera which was designed to provide a quantitative measure of the amount of noise that could be eliminated using this high frequency modulation technique. The next chapter discusses the imaging of fluorescently labeled mouse tumors. The role of this section is to demonstrate the camera acquiring fluorescent images and to show that the camera is capable of imaging fluorescently labeled dyes at concentrations that are safe for patients.

In order to quantitatively define the sensitivity of the camera to a fluorescence signal, the noise in the signal had to be measured. To do this a calibration was conducted in which the optical power equivalent of the noise was measured. This was done by measuring the

proportional response of the detector to light. Together with the amount of noise occurring in both the 1 MHz modulated and non-modulated images, the optical power equivalent of the noise for both images were calculated. These data show the improvement in the detection limit when the modulation technique is used and provides a lower limit for a detectable fluorescence signal.

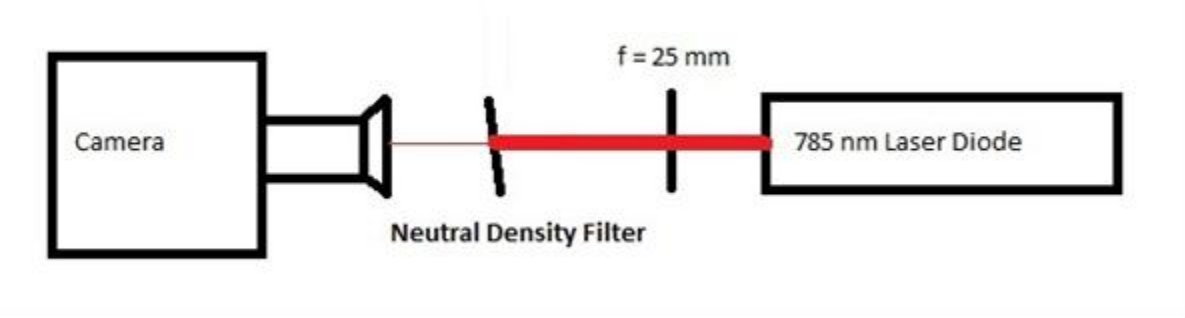

Figure 8: The Calibration Setup

In order to obtain the optical power equivalent of the noise in both the non-modulated and 1 MHz modulated signals from the camera, a method for calibrating the camera was developed (displayed in figure 8) The setup consisted of using a combination of neutral density filters and a 785 nm laser diode to create a variety of different low intensity laser beams with powers ranging from 25 to 300 nW. A wavelength of 785 nm was used because it was close to the wavelength of the fluorescent signal that we wished to detect and it is a commonly manufactured wavelength for inexpensive laser diodes. The laser diode was operated at 2 mW and was focused using a 25 mm focal length plano-convex lens. The beam then passed through a combination of neutral density filters positioned at approximately 10 degrees to the normal of the incident beam. The low intensity beam that emerged from the filters was approximately

1 cm in diameter when arriving at the camera. The beams ranged in power from 25 to 300 nW depending on the neutral density filters chosen. These powers were measured using a power meter consisting of a photodiode and a decade amplifier. This power range was chosen in order to ensure that the beam was not so intense that the pixels of the camera were saturated but not so low that the beam was hard to distinguish from the noise background that was acquired when the laser beam was blocked. The camera's built-in LEDs were disabled electronically and a band-pass filter (810-830 nm) that was installed by the company that manufactures the camera was removed so the 785 nm light could be detected. Even though the built-in LEDs were disabled, the fans attached to them were provided power in order to avoid thermal fluctuations. This resulted in a relatively consistent (± 10%) signal after one hour of operation which is when all calibration measurements were taken. All data were collected while the camera was in an optically shielded box in order to ensure the signal acquired was not contaminated by ambient light in the lab. A manual shutter was used to block the beam to provide a background signal.

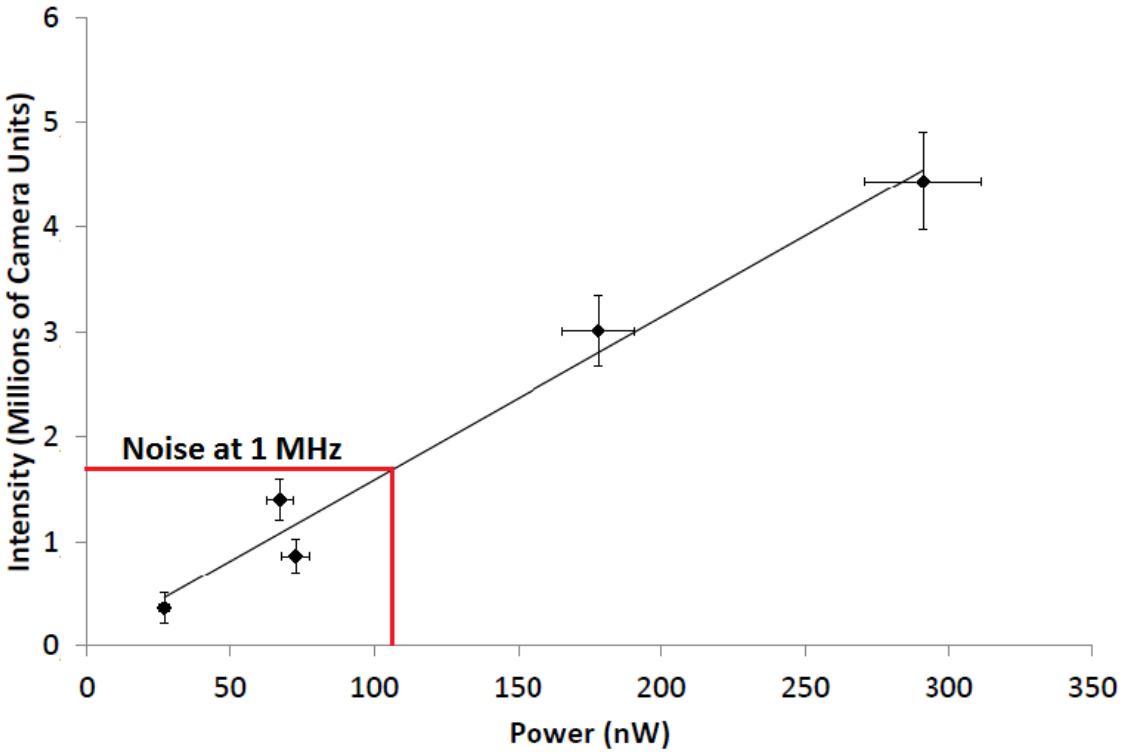

Figure 9: Graph of Calibration. The x-axis is the power of the filtered laser beam the camera was exposed to. The y-axis is the number of counts that the camera acquired when exposed to these beams minus the number of counts the camera acquired when the beam was blocked. The error bars represent an estimate of the first standard deviation of the uncertainty in each of the measurements. The black line is a linear least squares fit of the data which has an R squared value of 0.9771. The red line labeled "Noise at 1 MHz" corresponds to the total number of counts achieved in 50 ms at 1 MHz.

The results of the calibration are displayed in figure 9. In this calibration, each data point corresponds to a different optical power laser beam. Each measurement has an uncertainty from the power meter's measurement and the measurement of the number of counts

corresponding to the laser beam. One standard deviation estimates of these uncertainties are displayed in figure 10 as the error bars. The slope of the linear least squares fit of these data was used to obtain the number of counts per unit of light intensity. By inverting this quantity and multiplying by the number of counts achieved when the camera was optically shield, the optical power equivalent of the noise was acquired. For the 1 MHz modulated image the number of counts achieved was 1.7 ± 0.1 million (which is displayed as the red line in figure 9) and for the non-modulated image the number of counts was 800 ± 40 million (which is off the graph in figure 9). The optical power equivalents of the noise were then divided by the number of pixels (40k) to acquire the optical power equivalent of the noise per pixel. This measurement was done for both the signal acquired with a 1 MHz modulation and for the non-modulated signal to provide a comparison. The optical power equivalent per pixel was found to be 1.2 ± 0.1 nW for the non-modulated image and 2.6 ± 0.3 pW for the 1 MHz modulated image for a 50 ms integration time. This implies that the 1 MHz modulation technique has resulted in an over 400-fold improvement in the detection limit when compared to the non-modulated image and that for a signal to noise ratio of 1:1, the fluorescence signal must be 2.6 pW per pixel. The next chapter discusses how this 400-fold improvement was applied to imaging of fluorescently labeled mouse tumors.

V. Fluorescence Imaging

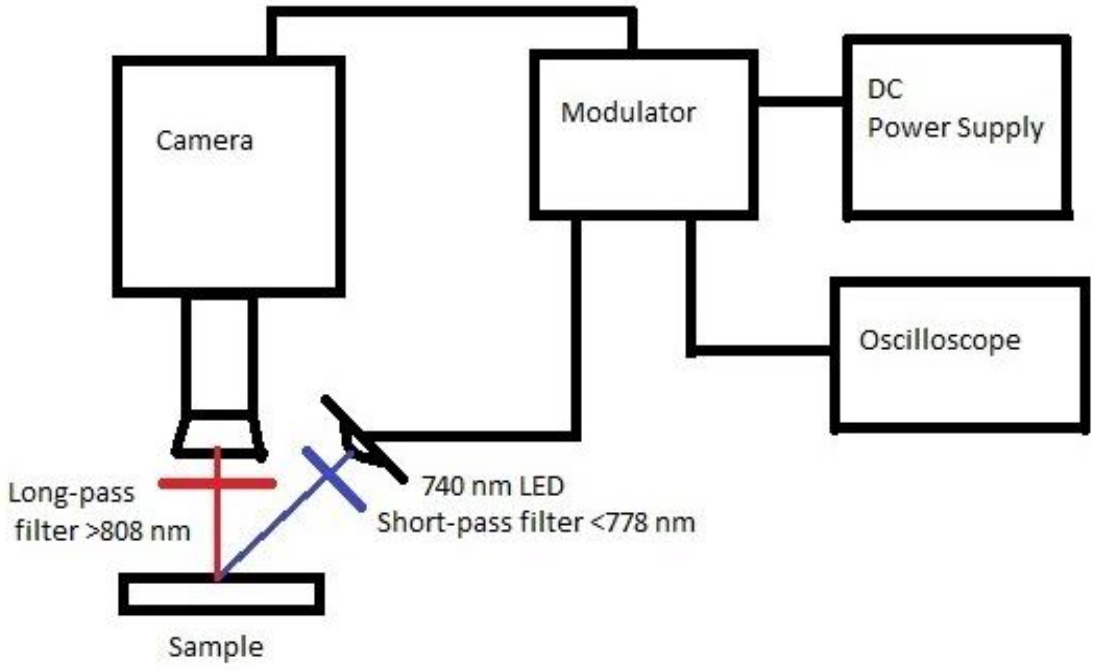

Figure 10: Fluorescence Imaging Setup

A setup quite different from the calibration setup was used in order to acquire fluorescence images. Like the previous setup, the built–in LEDs had to be disabled; however, in the fluorescence imaging setup, the electronic modulation signal emitted by the camera that previously went to these LEDs had to be electronically manipulated and used as an input to a different LED. This MHz modulated electronic signal was first sent to a home built modulator. The modulator allowed for control of the DC component of the modulation signal. As different wavelength LEDs operate at different voltages, being able to adjust this voltage was paramount for optimizing the signal for the ideal LED for exciting fluorescence. The AC signal should similarly need to be optimized; however, for the LED used the AC component of the signal at 1

MHz was so close to the optimal value that the slight improvement that could potentially be obtained was not worth pursuing with customized electronics. Using only a DC adjustment of 10.5 V, the current flow through the LED was measured to be a square wave with a minimum of no current and a maximum of 400 mAmps. As the recommended limit by the manufacturer of the LED was 600 mAmps, the potential marginal 200 mAmps was not seen as worth pursuing as configuring a circuit that could make an AC adjustment at such a high frequency is non-trivial.

The LED chosen for fluorescence imaging was a 1 W optical power 740 nm centered LED with a half-width of 30 nm. This LED was chosen because of its high optical power (to compete with the diffuse laser beams presently in use with current fluorescence imaging setups in the operating room[6]) and central wavelength near the absorption peak for the infrared fluorescent dye that was used as a fluorescent label.

The fluorescent dye used is known as IRDye 800CW. This dye is an organic molecule with a molecular weight of slightly over 1000 g/mol. [17] This dye is somewhat unusual among other fluorophores because its entire fluorescence pathway is in the near infrared as shown in Figure 11.

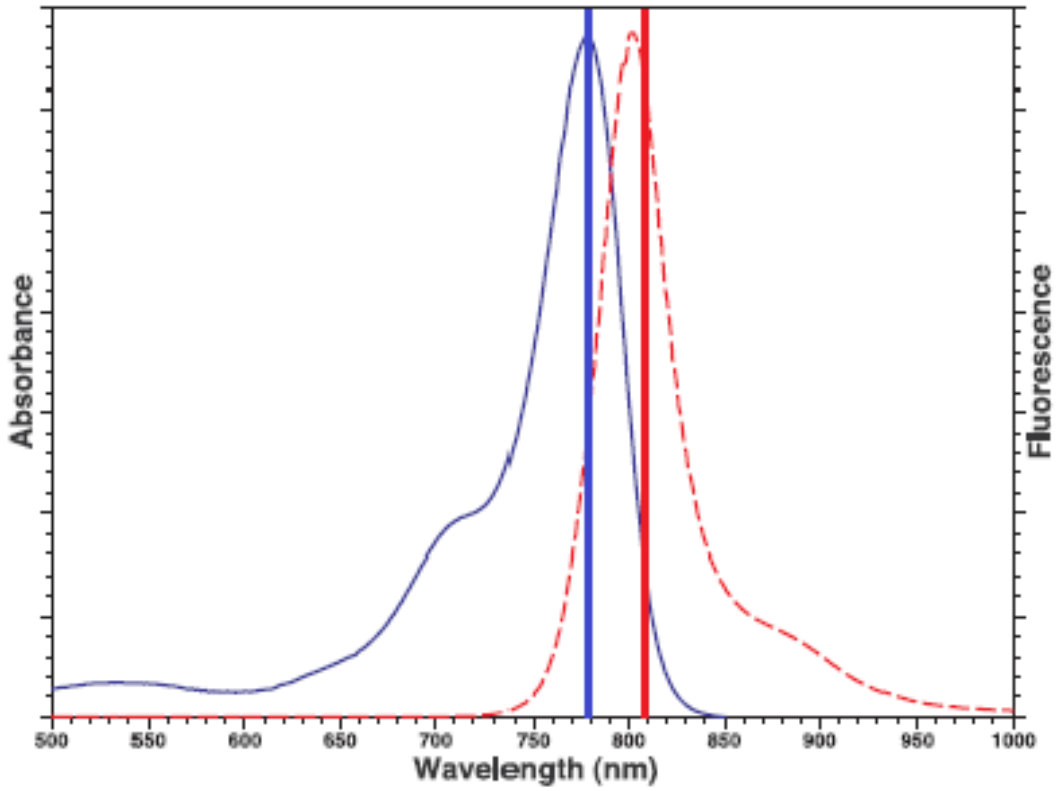

Figure 11: Fluorescence Absorption and Emission Spectra for CW 800 dye. The solid blue curve is the absorption spectrum. The dashed red curve is the emission spectrum. The vertical blue and red lines correspond to the cutoff wavelengths for the filters used in the apparatus described in figure 10. This figure is adapted from Reference 18.

In order to image mouse tumors labelled with a safe concentration of dyes, 6-8 week old mice were seeded with tumors. When the tumors grew to 6-8 mm in diameter, the mice were injected with 100 µg of IRDye 800CW. After 6 days the mice were sacrificed to maximize the concentration of the dye in the tumors. The tumors were then harvested and embedded in

paraffin wax.[19] This sample was then imaged using the setup shown in Figure 8. Three different tumors were imaged.

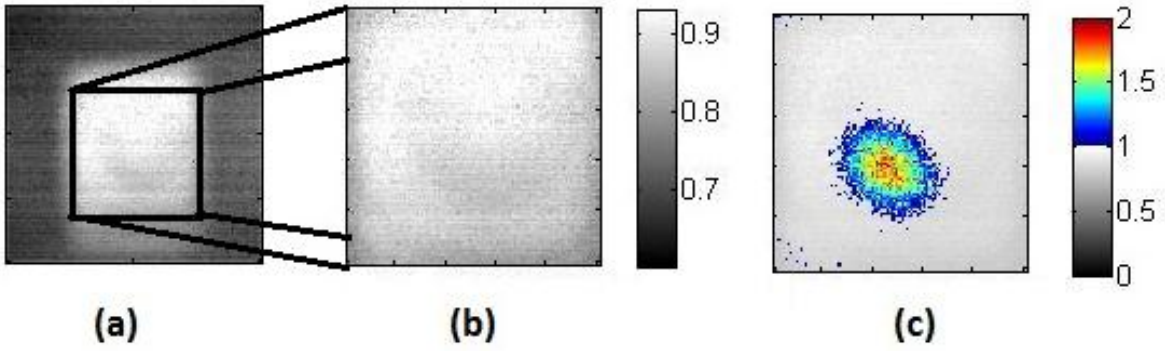

Figure 12: (a) full (200 by 200 pixels) non-modulated image of wax with mouse tumor. (b) Zoomed in (100 by 100 pixels) non-modulated image of the area near the tumor. (c) Image b with the 1 MHz modulated image of the tumor overlaid in color.

When the 1 MHz modulation technique was used to image mouse tumors labeled with fluorescent dye, the images in figure 12 were obtained. Figure 12 a and b show the non-modulated image. In these images only the paraffin wax the tumor is embedded in can be seen. If one looks closely at figure 12b, perhaps a faint hue of part of the tumor can be seen. However, if the 1 MHz image is examined (the color in figure 12c) the whole tumor can be clearly identified in the wax. Thus the tumor is almost entirely outside the detection limit of the non-modulated image, but well within the detection limit of the 1 MHz modulated image.

Therefore, this modulation technique has allowed for this camera to image tumors labeled with a physiologically safe amount of dye using only an LED as the light source.

VI. Conclusion

Imaging plays a pivotal role in treating cancer. Surgeons need to be able to identify tumors in order to remove them. Often smaller tumors cannot be identified by the human eye alone. The use of fluorescent dye labels and fluorescence imaging to identify these tumors is a new but promising technique for pushing the detection limit to smaller tumors. Furthermore, the use of infrared fluorescent dyes allows for imaging tumors embedded into the tissue. Because only a small quantity of dye can be injected into the patient safely, having an imaging device that is sensitive to the fluorescent signal of these dyes is paramount. One class of cameras originally developed for motion sensitive gaming applications that could provide this sensitive level of fluorescence imaging are time of flight cameras. Because these cameras are able to detect signals modulated at frequencies as high as 20 MHz using lock-in detection, they show great promise for eliminating lower frequency noise from a fluorescence image.

I have shown that by modulating at 1 MHz, the level of noise in the image can be reduced by more than 400-fold when compared to the non-modulated image when the camera is optically shielded. Subsequent studies[20] on this camera have shown that this more than 400-fold reduction is not dependent on modulating at MHz level frequencies as my original hypothesis indicated. Even at frequencies as low as 20 Hz, a similar level of noise reduction was

obtained. This implies shot noise dominates over 1/f noise at frequencies greater than 20 Hz in an optically shielded environment. Consequently the MHz level modulation is not necessary to lower the level of noise when the camera is optically shielded. However, when the camera is exposed to ambient light (light not being used to excite or being emitted by fluorescence), the detection limit is improved substantially by modulating at frequencies much higher than 20 Hz. The advantage over the non-modulated image can be seen in figure 12 as these images were taken in ambient light. Figure 5 supports that ambient light has components at frequencies above 20 Hz. Therefore, the MHz level modulation is useful for noise reduction when in the presence of ambient light, but not useful when the camera is optically shielded as a 20 Hz modulation results in the same level of noise. Since the proposed application is an endoscopic camera, this feature could prove useful as ambient light sources are likely to be present in the operating room.

Acknowledgments

I would like to thank a number of people for help with this project including: my research supervisors Herman Offerhaus Ph.D., Jennifer Herek Ph.D., and Erik Garbacik, my honors thesis and senior experience advisor Jeffrey Collett Ph.D., Jeroen Korterik and Frans Segerink for technical support with the experiment, my collaborators Wouter Nagengast M.D. Ph.D. and Marlous Arjaans M.D. at the University Medical Center of Groningen for providing the mouse tumors, LU-R1 and the University of Twente for funding, Kathlene Kuisv D.O. for finding and providing medical literature, and Barbara Kusiv for proof reading the manuscript.

References

(1) Akiba, N.; Saitoh, N.; Kuroki, K.; Igarashi, N.; Kurosawa, K. Visualizing Latent Fingerprints on Color-Printed Papers Using Ultraviolet Fluorescence. *J. Forensic Sci.* **2011***, 56*, 754-759.

(2) Esposito, A.; Oggier, T.; Gerritsen, H.; Lustenberger, F.; Wouters, F. All-solid-state lock-in imaging for wide-field fluorescence lifetime sensing RID A-8536-2008 RID B-6303-2008. *Opt. Express* **2005***, 13*, 9812-9821.

(3) Grotjohann, T.; Testa, I.; Leutenegger, M.; Bock, H.; Urban, N. T.; Lavoie-Cardinal, F.; Willig, K. I.; Eggeling, C.; Jakobs, S.; Hell, S. W. Diffraction-unlimited all-optical imaging and writing with a photochromic GFP. *Nature* **2011***, 478*, 204-208.

(4) Li, G.; Xie, X. S. Central dogma at the single-molecule level in living cells RID E-7657-2010. *Nature* **2011***, 475*, 308-315.

(5) Cassidy, J.,; Bissett, D.; Spence, R. A. J.; NetLibrary, I. In *Oxford handbook of oncology [electronic resource];* Oxford University Press: Oxford ; New York :, 2002; pp 418.

(6) van Dam, G. M.; Themelis, G.; Crane, L. M. A.; Harlaar, N. J.; Pleijhuis, R. G.; Kelder, W.; Sarantopoulos, A.; de Jong, J. S.; Arts, H. J. G.; van der Zee, A. G. J.; Bart, J.; Low, P. S.; Ntziachristos, V. Intraoperative tumor-specific fluorescence imaging in ovarian cancer by folate receptor-alpha targeting: first in-human results. *Nat. Med.* **2011***, 17*, 1315-U202.

(7) Cukier, D.; NetLibrary, I. In *Coping with chemotherapy and radiation [electronic resource] / Daniel Cukier ... [et al.];* McGraw-Hill: New York :, 2005; pp 28, 35 and 37-38.

(8) Gardner, E. K. Purdue technology used in first fluorescence-guided ovarian cancer surgery. http://www.purdue.edu/newsroom/research/2011/110918LowSurgery.html (accessed 02/17, 2011).

(9) Terwisscha van Scheltinga, A. G. T.; van Dam, G. M.; Nagengast, W. B.; Ntziachristos, V.; Hollema, H.; Herek, J. L.; Schroder, C. P.; Kosterink, J. G. W.; Lub-de Hoog, M. N.; de Vries, E. G. E. Intraoperative near-infrared fluorescence tumor imaging with vascular endothelial growth factor and human epidermal growth factor receptor 2 targeting antibodies. *Journal of nuclear medicine : official publication, Society of Nuclear Medicine* **2011***, 52*, 1778-1785.

(10) Schlaerth, A.; Abu Rustum, N. Role of minimally invasive surgery in gynecologic cancers. *Oncologist* **2006***, 11*, 895-901.

(11) Azziz, R.; Murphy, A.; Steinkampf, M. P. Postoperative recuperation: relation to the extent of endoscopic surgery. *Fertil. Steril.* **1989***, 51*, 1061-1064.

(12) Bilton, N. Video Game Industry Continues Major Growth, Gartner Says. *New York Times* **July 5th 2011**.

(13) Foix, S.; Alenya, G.; Torras, C. Lock-in Time-of-Flight (ToF) Cameras: A Survey. *IEEE Sens. J.* **2011***, 11*, 1917-1926.

(14) PMD Technologies LightVis User Manual Version 1.1. **2010**, 4.

(15) Vanderziel, A. Unified Presentation of 1/f Noise in Electronic Devices - Fundamental 1/f Noise Sources. *Proc IEEE* **1988***, 76*, 233-258.

(16) Lackowitz, J. R. In *Principles of Fluorescence Spectroscopy;* Springer: New York, 2006; pp 175-180.

(17) Li-Cor Corporation **IRDye® 800CW Carboxylate**. http://www.licor.com/bio/products/reagents/irdye_800cw_nhs_ester/irdye_800cw_nhs_ester.jsp (accessed 04/22, 2012).

(18) Nagengast, W. B. Department of Medical Oncology, University Medical Center Groningen, The Netherlands. Personal Communication, July, 2011.

(19) Arjaans, M.; Nagengast, W. Department of Medical Oncology, University Medical Center Groningen, The Netherlands. Personal Communication, December 2011.

(20) Korterik, J.; Offerhaus, H. Department of Applied Physics, University of Twente, Enschede, The Netherlands. Personal Communication, April 2012.

Appendix

Derivation of Lock-in detection noise response for a square wave modulation.

If we let τ be the modulation period and the noise function be an arbitrary function of omega where

$$N(t) = \int_{-\infty}^{\infty} N(\omega) e^{i\omega t} d\omega$$

Then net noise detected over N cycles will be the difference between the integral over the first half of the modulation period and the integral over the second half of the modulation period.

$$I_{noise} = \int_{-\infty}^{\infty} \left[\sum_{j=-\frac{N}{2}}^{\frac{N}{2}} \left[\int_{j\tau}^{\left(j+\frac{1}{2}\right)\tau} N(\omega) e^{i\omega t} dt - \int_{\left(j+\frac{1}{2}\right)\tau}^{(j+1)\tau} N(\omega) e^{i\omega t} dt \right] \right] d\omega$$

By factoring out a phase shift term from the second integral with respect to t, both integrals with respect to t can be combined.

$$I_{noise} = \int_{-\infty}^{\infty} \left[\sum_{j=-\frac{N}{2}}^{\frac{N}{2}} \left[\int_{j\tau}^{\left(j+\frac{1}{2}\right)\tau} N(\omega) e^{i\omega t} \left[1 - e^{\frac{i\omega\tau}{2}} \right] dt \right] \right] d\omega$$

By integrating with respect to t

$$I_{noise} = \int_{-\infty}^{\infty} \left[\sum_{j=-\frac{N}{2}}^{\frac{N}{2}} \left[\frac{N(\omega)}{i\omega} \left[e^{i\left(j+\frac{1}{2}\right)\tau} - e^{ij\omega\tau} \right] \right] \right] d\omega$$

This is algebraically equivalent to

$$I_{noise} = \int_{-\infty}^{\infty} \left[\frac{N(\omega)}{i\omega} \left[1 - e^{\frac{i\omega\tau}{2}} \right] \left[e^{-\frac{i\omega\tau}{2}} - e^{-i\omega\tau} \right] \sum_{j=\frac{-N}{2}}^{\frac{N}{2}-1} e^{ij\omega\tau} \right] d\omega$$

The sum at the end of the integrand is a geometric series allowing for the expression to be written as

$$I_{noise} = \int_{-\infty}^{\infty} \left[\frac{N(\omega)}{i\omega} \left[1 - e^{\frac{i\omega\tau}{2}} \right] \left[e^{-\frac{i\omega\tau}{2}} - e^{-i\omega\tau} \right] \frac{e^{i\omega\tau} \left[e^{-\frac{iN\omega\tau}{2}} - e^{\frac{-N}{2}i\omega\tau} \right]}{1 - e^{i\omega\tau}} \right] d\omega$$

This is algebraically equivalent to

$$I_{noise} = \int_{-\infty}^{\infty} \left[\frac{4N(\omega)}{i\omega} e^{\frac{i\omega\tau}{2}} \sin^2\left(\frac{\omega\tau}{4}\right) \frac{\sin\left(\frac{N\omega\tau}{2}\right)}{\sin\left(\frac{\omega\tau}{2}\right)} \right] d\omega$$